A progressive damage simulation algorithm for GFRP composites under cyclic loading. Part I: Material constitutive model

Elias N. Eliopoulos, Theodore P. Philippidis

A progressive damage simulation algorithm for GFRP composites under cyclic loading. Part I: Material constitutive model

Elias N. Eliopoulos, Theodore P. Philippidis

PII: S0266-3538(11)00051-0
DOI: 10.1016/j.compscitech.2011.01.023
Reference: CSTE 4918

To appear in: *Composites Science and Technology*

Received Date: 19 August 2010
Revised Date: 24 January 2011
Accepted Date: 30 January 2011

Please cite this article as: Eliopoulos, E.N., Philippidis, T.P., A progressive damage simulation algorithm for GFRP composites under cyclic loading. Part I: Material constitutive model, *Composites Science and Technology* (2011), doi: 10.1016/j.compscitech.2011.01.023

A progressive damage simulation algorithm for GFRP composites under cyclic loading.

Part I: Material constitutive model

Elias N. Eliopoulos, Theodore P. Philippidis[1]

Department of Mechanical Engineering & Aeronautics, University of Patras

P.O. Box 1401, GR 26504 Panepistimioupolis, Rio, Greece

Abstract

A life prediction algorithm and its implementation for a thick-shell finite element formulation for GFRP composites under constant or variable amplitude loading is introduced in this work. It is a distributed damage model in the sense that constitutive material response is defined in terms of meso-mechanics for the unidirectional ply. The algorithm modules for non-linear material behaviour, pseudo-static loading-unloading-reloading response, constant life diagrams and strength and stiffness degradation due to cyclic loading were implemented on a robust and comprehensive experimental database for a unidirectional Glass/Epoxy ply. The model, based on property definition in the principal coordinate system of the constitutive ply, can be used, besides life prediction, to assess strength and stiffness of any multidirectional laminate after arbitrary, constant or variable amplitude multi-axial cyclic loading. Numerical predictions were corroborated satisfactorily by test data from constant amplitude fatigue of Glass/Epoxy laminates of various stacking sequences.

Keywords: Polymer-matrix composites (PMCs) (A), Fatigue (B), Damage mechanics (B), Finite element analysis (FEA) (C), Life prediction (D)

[1] Corresponding author: e-mail: philippidis@mech.upatras.gr, Tel. +30-2610-969450, 997235, Fax: +30-2610-969417

1 Introduction

Life prediction and stress analysis for structures made of composite laminates under variable amplitude multiaxial cyclic loads still remain an open issue. For structural composite parts of the aeronautical, naval and wind turbine rotor blade industries, among others, elastic stability and fatigue constitute the dominant analyses for design and dimensioning. Even in structures where ultimate load design cases are predominant, verification of fatigue strength and life prediction are prerequisite for design approval and certification purposes.

For damage tolerant design considerations, the effect of local failure and stiffness degradation due to cyclic loading, causing stress redistribution, should be investigated. As the complicated geometry of the real structure and the existence of multiple confined domains in its volume with different in essence mechanical properties render the analytical stress and strain calculations impossible, a numerical method, e.g. finite elements (FE) is in order.

There are relatively few works published on the subject, most of them in the last two decades. Based on the *Internal State Variable Approach* of Lee et al. [1], Harris and co-workers [2]-[3] have presented possibly the first contribution in the field. The approach followed by Harris and co-workers is of the "ply-to-laminate" type in which all constitutive formulation takes place at the ply level. Prediction of life, strength or stiffness for a laminate of any stacking sequence, composed of the building ply is in general possible. Perhaps, the most complete work of that type of approach was published by Shokrieh and Lessard [4]-[5], based however, on linear material response.

In the present work, a continuum damage mechanics method is implemented in a *ply-to-laminate* life prediction scheme for composite laminates under cyclic loading. As a result of failure onset driven by the stress at a point, a set of appropriate stiffness degradation rules is applied, resulting in a modified stiffness tensor, typical of the damaged medium. This effective medium description requires besides *sudden stiffness* degradation, gradual strength and stiffness degradation as well due to cyclic load, expressed as a function of the number of cycles, n. It certainly requires an important experimental effort, besides efficient modelling, to cover the various loading conditions, e.g. tension-tension (T-T), tension-compression (T-C), etc., at various stress ratio, R, values and material principal directions.

To assess conditions of incipient failure in a specific mode, compatible with certain defect type and respective stiffness degradation strategy, the failure criteria by Puck [6]-[7], were implemented.

The material model consists also of the detailed description of fatigue strength in each principal material direction and in-plane shear, for several R values to ease the implementation of Constant Life Diagram (CLD) formulations.

A detailed load step-by-step simulation of each cycle is foreseen in the realization of the algorithm. Non-linear material response of the unidirectional (UD) ply is taken into account, introducing appropriate models derived by fitting experimental data. In the numerical analysis, non-linearity is modelled by implementing a piece-wise linear incremental stress-strain constitutive law.

The algorithm is implemented for various element formulations of a commercial FE code. Results of an earlier development stage of the method by means of FE were presented by Philippidis et al. [8]. A version of the algorithm considering homogenous stress fields and proceeding by means of Classical Lamination Theory (CLT) assumptions was presented by Philippidis and Eliopoulos [9], predicting the mechanical behaviour of multidirectional (MD) laminates subjected to various loading conditions. An earlier linear version of the method, considering also homogenous stress fields, was presented by Passipoularidis et al. [10]. An extensive comparison of life prediction, strength and stiffness degradation numerical results with experimental data, validating thus the proposed algorithm, was presented in the second part of this work [11].

2 Constitutive Laws

The progressive damage simulator for life prediction under cyclic complex stress presented in this work was devised for Glass/Epoxy composites typical of those used in the wind turbine rotor blade industry. It relies on material data from a huge experimental effort in the frame of an EC-funded research project that resulted in a comprehensive material property database with test results from static, cyclic and residual strength experiments under axial and multi-axial loading conditions. All data are free for download (http://www.wmc.eu/optimatblades.php) in the official OPTIMAT BLADES site along with the relevant reports.

2.1 Ply response under quasi-static monotonic loading

The basic building block of all laminates considered is the Glass/Epoxy UD ply. Characterization of constituent fibre and matrix materials along with cured composite technical characteristics, e.g. fibre volume fraction, glass transition temperature etc. were reported in [12]. Static tests were performed both parallel and transverse to the

fibres and also in shear. Most of the data were also published by Antoniou et al. [13]. The in-plane shear strength was obtained through v-notched Iosipescu tests; see Megnis and Brøndsted [14].

To take into account the highly non-linear material behaviour observed transversely to the fibres, mainly in compression and under in-plane shear, incremental stress-strain equations were implemented, retaining the validity of the generalized Hooke law for each individual interval:

$$\begin{aligned} d\sigma_1 &= \frac{E_1}{1-\frac{E_{2t}}{E_1}\nu_{12}^2}d\varepsilon_1 + \frac{\nu_{12}E_{2t}}{1-\frac{E_{2t}}{E_1}\nu_{12}^2}d\varepsilon_2 \\ d\sigma_2 &= \frac{\nu_{12}E_{2t}}{1-\frac{E_{2t}}{E_1}\nu_{12}^2}d\varepsilon_1 + \frac{E_{2t}}{1-\frac{E_{2t}}{E_1}\nu_{12}^2}d\varepsilon_2 \\ d\sigma_6 &= G_{12t}d\varepsilon_6 \end{aligned} \tag{1}$$

In the above equations, E_1 and ν_{12} were considered constant up to failure, while the tangential elastic moduli E_{2t} and G_{12t} were given by the nonlinear constitutive relation introduced by Richard and Blacklock [15]:

$$E_{2t} = \frac{d\sigma_2}{d\varepsilon_2} = E_{o_2}\left[1-\left(\frac{\sigma_2}{\sigma_{o_2}}\right)^{n_2}\right]^{\frac{1}{n_2}+1} \quad G_{12t} = \frac{d\sigma_6}{d\varepsilon_6} = G_{o_{12}}\left[1-\left(\frac{\sigma_6}{\sigma_{o_6}}\right)^{n_6}\right]^{\frac{1}{n_6}+1} \tag{2}$$

The parameters $E_{o_2}, \sigma_{o_2}, n_2$ were found different in tension and compression [13]. Numerical values for all the above constants were summarized in Table 1. Mean values of the ply in-plane failure stresses were given in Table 2. By X, Y and S the respective strengths in the fibre direction, transversely and in-plane shear were denoted. All numerical values of Tables 1 and 2 were derived from data of at least 25 coupon tests per mechanical property.

Table 1 Elastic constants (in MPa). OB_UD Glass/Epoxy

E_1=37,950 ν_{12}=0.28

	E_{o_i}	σ_{o_i}	n_i
$E_{2t}^{(T)}$	15,035	75	3
$E_{2t}^{(C)}$	15,262	188	2.18
G_{12t}	5,500	67	1.3

Table 2 Failure stress (in MPa). OB_UD Glass/Epoxy

X_T	X_C	Y_T	Y_C	**S**
776	686	54	165	80

2.2 Loading-Unloading-Reloading (L-U-R)

Engineering elastic constants appearing in the constitutive relations, Eq. (1), are valid for monotonic loading conditions. Upon unloading, the stiffness changes and must be again defined experimentally. It was further observed that stiffness decreases upon repeated L-U-R cycles, depending on the stress level previously reached. As reported by Philippidis et al. [8], the stiffness reduction is more severe for matrix dominated response, e.g. in-plane shear and transverse loading to the fibres, see Fig. 1. Stiffness reduction due to L-U-R cycles when loading parallel to the fibres was negligible.

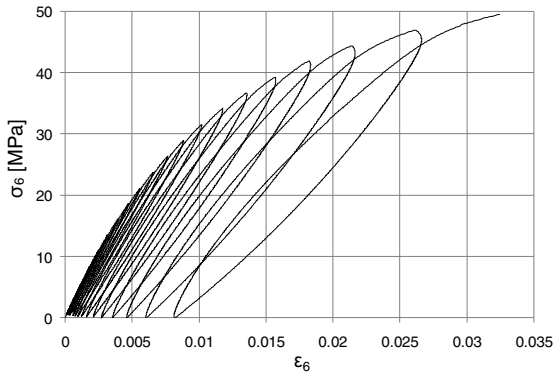

Fig. 1: Typical shear stress-strain cycles under static L-U-R

This type of stiffness degradation was measured by means of dedicated experiments performed in the frame of this work; ISO 14129 coupons of $[\pm 45]_S$ lay-up were used for the in-plane shear tests while the OB (OPTIMAT BLADES) coupon geometry was adopted for transverse to the fibres tensile and compressive tests. Strain was recorded during the L-U-R tests using strain gauges. The elastic modulus was determined as the slope of the linear regression model of each stress-strain loop. The values from a test were normalized with respect to the modulus of the first cycle and plotted vs. the normalized (with respect to the nominal strength value) stress level, see Fig. 2.

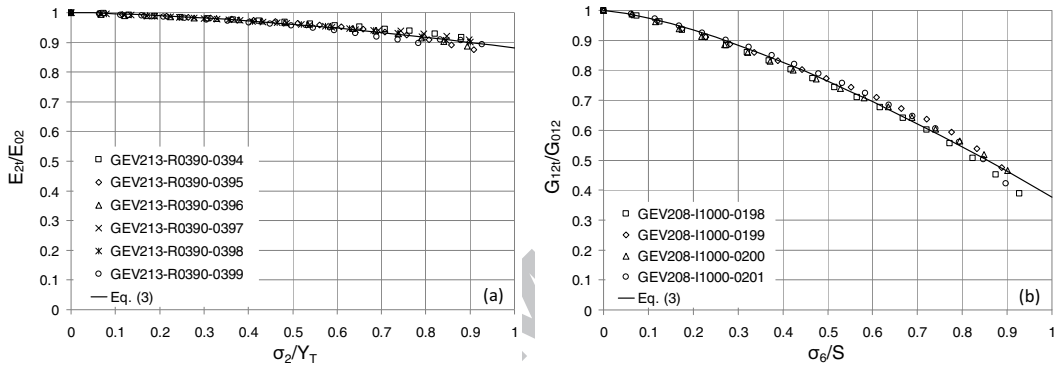

Fig. 2: Modulus degradation due to L-U-R cycles. (a) Transverse in tension (b) In-plane shear

The stiffness degradation models were determined with nonlinear regression applied on the normalized stiffness-stress data from all tests and given by:

$$\frac{E_{2t}}{E_{o_2}} = 1-(1-a_2)\left(\frac{\sigma_2}{Y_T}\right)^{b_2},\ \frac{G_{12t}}{G_{o_{12}}} = 1-(1-a_6)\left(\frac{\sigma_6}{S}\right)^{b_6} \quad (3)$$

where Y_T and S stand for the tensile strength transversely to the fibres and in-plane shear strength respectively derived from tests on the ISO 14129 coupons. Since values of E_{o_2} or $G_{o_{12}}$ presented slight variations for the different coupon tests, the respective values from Table 1 were implemented along with Eq. (3). The parameters a_2, b_2 were found

different in tension and compression. Numerical values for all the above constants were summarized in Table 3.

Table 3: Parameter values for L-U-R stiffness degradation models, Eq. (3)

	a_i	b_i
$E_{2t}^{(T)}$	0.88	1.60
$E_{2t}^{(C)}$	0.65	2.77
G_{12t}	0.38	1.40

When the first of Eq. (3) is used to determine the compressive elastic modulus transverse to the fibres, the tensile strength, Y_T, should be replaced by the corresponding compressive one, Y_C.

2.3 Progressive Stiffness Degradation

In-plane stiffness of the lamina is degrading due to several reasons, e.g. *sudden stiffness* reduction due to some kind of failure occurrence or progressive stiffness reduction due to cyclic loading. In general, the latter is non linear and several formulations were proposed in the literature to describe it. As presented by Philippidis et al. [8], during constant amplitude (CA) cyclic tests [16]-[17], load-displacement data corresponding to ca. 10 cycles were recorded periodically and were transformed to respective stress-strain data, e.g. see Fig. 3a where experimental data from CA cyclic loading of a $[90_7]_T$ coupon at a stress ratio R=-1 (T-C) were shown. The calculated strain was proved to be accurate by comparing with extensometer data for low stiffness specimens as of [16]-[17] where no tab debonding occurred during the test. The stiffness of the coupon at the first cycle of each periodically recorded block of cycles was determined as the slope of the linear regression model of the respective stress-strain loop. These stiffness values were normalized with respect to the stiffness of the first cycle and plotted vs. the normalized number of cycles with respect to the number of cycles at failure. For

example, for the case of a $[90_7]_T$ coupon, said results from all available stress levels at R=0.1 and -1 were presented in Fig. 3b. Due to the high experimental scatter it was thought more appropriate to select a representative group of data for fitting the material model, e.g. in Fig 3b the solid line data corresponding to R=-1 and stress level of 24.3 MPa were chosen for the tensile transverse modulus. The stiffness degradation models were determined with nonlinear regression applied on the normalized stiffness-cycle number data from these representative load cases, Fig. 4a. A similar procedure was also followed to derive the compressive modulus degradation shown in Fig. 4b and the respective one for the in-plane shear modulus.

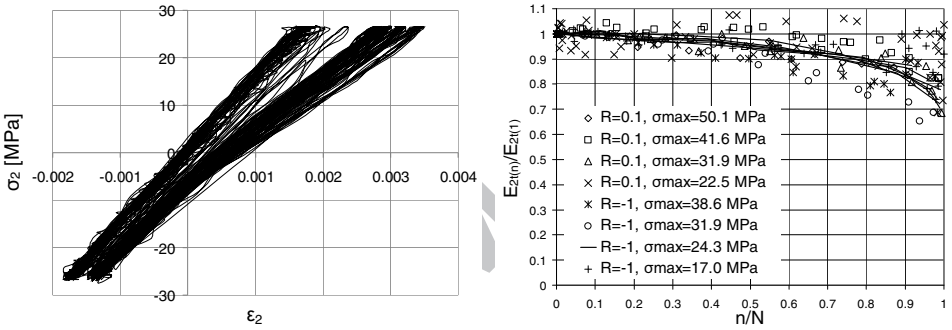

Fig. 3: (a) Stress-strain cycles under R=-1 CA fatigue transversely to the fibres, (b) Respective stiffness degradation data from R=0.1 and -1

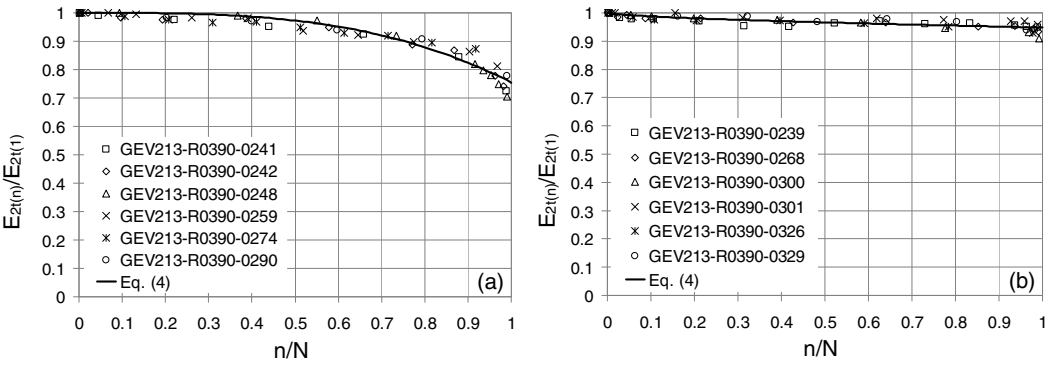

Fig. 4: Transverse modulus degradation due to CA cyclic loading

(a) Tensile (b) Compressive

In the present FADAS implementation the regression models depend only on the fatigue life fraction, i.e. the ratio of the applied cycles versus the nominal fatigue life at the current stress level. In this way, the modulus degradation depends implicitly also on the stress ratio, R, and the maximum applied cyclic stress, σ_{max}. The following functional forms were fitted to the experimental data:

$$\frac{E_{2t}(n)}{E_{2t}(1)} = 1-(1-c_2)\left(\frac{n}{N}\right)^{d_2},\ \frac{G_{12t}(n)}{G_{12t}(1)} = 1-(1-c_6)\left(\frac{n}{N}\right)^{d_6} \quad (4)$$

The parameters c_2, d_2 were found different in tension and compression; they were calculated by fitting test data from 6 tests at R=-1 and σ_{max}=24.3 MPa for the tensile E_{2t} and from 6 tests at R=10 and σ_{min}=-138.6 MPa for the compressive E_{2t}. For the in-plane shear modulus, G_{12t}, 5 tests on ISO 14129 coupons of $[\pm 45]_S$ lay-up at σ_{max}=63.6 MPa and 5 tests at σ_{max}=48.5 MPa, R=0.1, were used together as they exhibited similar stiffness degradation [9]. Numerical values for all the above constants were presented in Table 4. Since the modulus values at the first cycle from the different coupons tested were different, $E_{2t(1)}$ and $G_{12t(1)}$ in Eq. (4) were substituted by the respective, to the stress level, reloading stiffness values as given by Eq. (3).

For CA testing in the fibre direction, axial strain was measured with extensometers in 4 UD coupons [18]. Description of this type of tests can be found in [19]. Progressive stiffness degradation during cyclic loading parallel to the fibres was not important (1-2%), as shown in Fig. 5 and thus it was neglected in the numerical model.

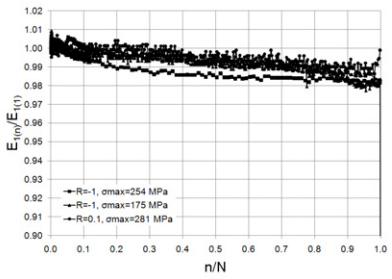

Fig. 5: Stiffness degradation of the UD ply in the fibres direction due to CA loading

Table 4: Parameter values for the progressive stiffness degradation models, Eq. (4)

	c_i	d_i
$E_{2t}^{(T)}$	0.75	3.17
$E_{2t}^{(C)}$	0.95	0.62
G_{12t}	0.68	1.65

2.3.1 Pre-failure Material Models

In case that no failure was detected in an integration point, the simulated ply response and especially the description of stiffness evolution for VA cyclic loading were expressed by combining the constitutive relations presented in the above. For each stress tensor component at the k-th loading step it is examined if it corresponds to loading, i.e. $\left|\sigma_{i(k)}\right| \geq \left|\sigma_{i(k-1)}\right|$, i=1, 2, 6 or else to unloading.

In the former case, if $\sigma_{i(k)}$ is higher than the global maximum stress, $\sigma_{i_{G\max}}$ or lower than the global minimum stress, $\sigma_{i_{G\min}}$, the initial material behaviour under quasi-static loading, presented in section 2.1 is assumed. That is, constant modulus E_1 and Poisson ratio v_{12} while E_{2t} and G_{12t} are functions of $\sigma_{2(k)}$ and $\sigma_{6(k)}$ as expressed by Eq. (2). If $\sigma_{i(k)}$ lies between the global minimum and maximum stress, the material response is assumed linear elastic while the reload elastic properties are used, Eq. (3), calculated at the global maximum or minimum stress, degraded according to the stiffness reduction models due to cyclic loading, i.e. Eq. (4).

In the case of unloading, elastic properties slightly higher than in reloading were introduced to account for an increasing permanent strain due to cyclic loading. In the

routine this is realized by multiplying by a number slightly higher than one the reloading stiffness values for E_{2t} and G_{12t}. The specific value depends on the numerical implementation, see comments in Part II [11].

The above was illustrated in Fig. 6:

A-B: Initial loading. Stress is always greater than its previous global maximum value, so the non-linear material behaviour under quasi-static loading is used.

B-C-D: Stress cycling under CA or VA. Stress values remain between their global minimum and maximum values, 0 and σ_{iGmax} respectively, so the reload and unload elastic properties were used, gradually degrading with increasing number of cycles.

D-E: Stress becomes greater than its previous global maximum value σ_{iGmax}, so the initial material behaviour is assumed etc.

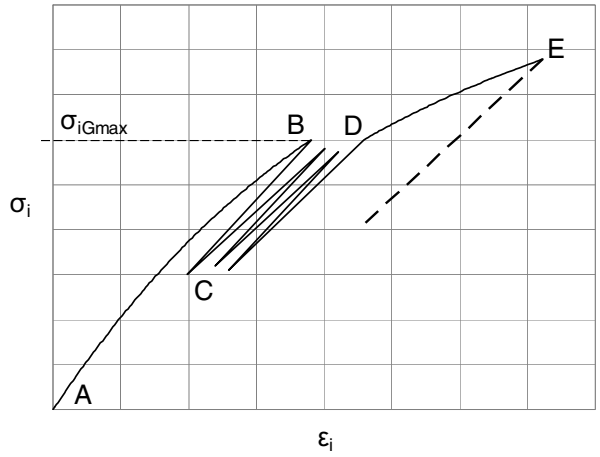

Fig. 6: Pre-failure material model for the UD Glass/Epoxy

2.3.2 Post-failure Material Models

Upon failure onset in some loading step, the stiffness degrades depending on the failure mode observed and the changes apply for the next loading step. If fibres break under either tensile or compressive stress, the three engineering elastic constants, E_1, E_{2t} and

G_{12t} drop to zero. If matrix damage modes occur, also called inter-fibre failure (IFF) by Puck [6]-[7], then only E_{2t} and G_{12t} drop to zero.

After fibres failure (FF), the unload behaviour for all three stress tensor components remains as in the material without failure, see section 2.3.1. If reloading occurs before any stress tensor component has changed sign, the respective modulus, i.e. E_1, E_{2t}, or G_{12t} drops to zero. If the stress has changed sign once, the corresponding modulus remains always at zero. The above was illustrated in Fig. 7:

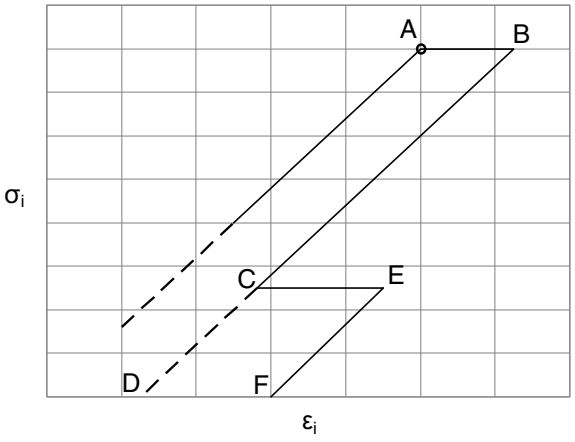

Fig. 7: Post-FF material model for the UD Glass/Epoxy

A: Stress level at which FF mode was detected.

A-B: If $\sigma_{i(k)}$ stands for loading, the corresponding engineering elastic constant drops to zero.

B-C, C-D, E-F: Unloading using the unloading elastic properties.

C-E: If reloading is encountered before stress has changed sign, the elastic property drops to zero.

D, F: Following unloading a stress tensor component changes sign. The corresponding elastic property drops and remains henceforth at zero.

In case of matrix failure, IFF damage modes, E_1 remains unaffected and only the normal stress transverse to the fibres and the in-plane shear component are taken into account in the stiffness degradation model.

Once IFF has occurred, the material is assumed to retain both its unload and reload properties as for the undamaged material, i.e. given by Eq. (3), (4), provided that the stress components σ_2 or σ_6 remain below its previous values at failure or IFF is not detected again. In the latter case, both engineering elastic constants E_{2t} and G_{12t} are set to zero. If however only the value of the normal stress transverse to the fibres σ_2 or the in-plane shear stress σ_6 exceeds its value for which IFF has been predicted last time, the respective elastic property drops to zero (E_{2t} or G_{12t}) and the process is continued. With respect to Fig. 8, illustrating the above, the following characteristics can be noted.

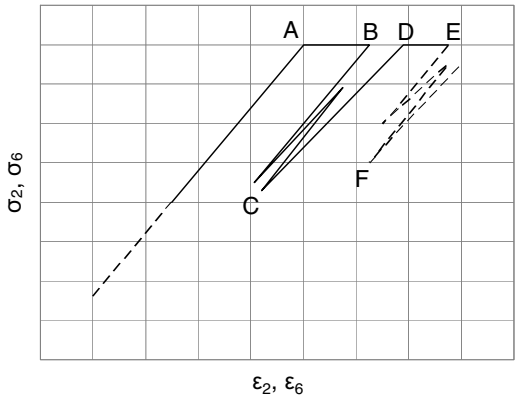

Fig. 8: Post-IFF material model for the UD Glass/Epoxy

A: Stress level at which IFF was first detected.

A-B: Loading is continued; both E_2 and G_{12} drop to zero.

B-C-D: No IFF is predicted again. Stress component remains lower than its value at failure. The reload and unload elastic properties of the undamaged material are used, gradually degraded with the number of cycles.

D-E: IFF is predicted once more or stress σ_2 or σ_6 becomes equal or greater than its value when IFF was predicted. The corresponding elastic property drops to zero.

E-F: The process is continued and the elastic properties are set again to its undamaged values for stress cycles of lower max values than previously.

3 Strength Degradation due to cyclic loading

Static strength degradation or residual strength after fatigue in composites has been intensively investigated the last 30 years. Numerous research groups have developed a variety of models; an appraisal of their effectiveness has been recently presented by Philippidis and Passipoularidis [20].

From the processing of the experimental data, the main conclusions were derived and formulated as guidelines for further development [21]. First, the residual strength in both principal material directions of the UD Glass/Epoxy is not affected when cyclic stress of the opposite sign is applied, i.e. tensile strength is not reduced under purely compressive cycles and vice versa. A similar trend was also observed by Nijssen [22] from tests on a fibre dominated MD laminate made of the same UD Glass/Epoxy material.

The tensile and the in-plane shear static strength experienced degradation of up to 40% when tested at a nominal life fraction of 80% [20]-[21]. The compressive residual strength on the other hand did not show significant degradation in all types of loading and material directions. Concerning the many theoretical models considered in [20], it was demonstrated in a clear manner that the complexity of a model is not related to the accuracy of its predictions [21]. In addition, it was also proved that life prediction

results under VA loading were not very sensitive to which residual strength model, of those examined was used as damage metric [23].

Therefore, the models used herein to describe the phenomenon are two: For the modelling of tensile residual strength along the principal material directions, under T-T or T-C cyclic loading, as well as of in-plane shear strength, the linear degradation model proposed by Broutman & Sahu [24] was implemented. Besides being the simplest one available, it requires no residual strength testing while at the same time it has been proven to produce always safe residual strength predictions under various stress conditions and lay-ups [23].

The compressive strength, both parallel and transversely to the fibres has been shown not to degrade significantly due to fatigue, especially when the specimens were subjected to tensile cyclic stress. Nevertheless, in modelling the compressive residual strength under C-C or T-C cyclic loading, a degradation equation simulating constant strength throughout the life with a sudden drop near failure (sudden death) was implemented.

According to the above observations the residual strength model in the principal coordinate system of the unidirectional glass/epoxy layer due to cyclic loading is given by a different set of equations, depending on the value of the cyclic stress ratio, R. The following set of equations is valid for $0 \le R < 1$:

$$X_{T_r} = X_T - (X_T - \sigma_{1max})\left(\frac{n}{N_1}\right),\ X_{C_r} = X_C, \qquad Y_{T_r} = Y_T - (Y_T - \sigma_{2max})\left(\frac{n}{N_2}\right),\ Y_{C_r} = Y_C$$

$$S_r = S - (S - \sigma_{6max})\left(\frac{n}{N_6}\right). \tag{5}$$

For $-1 \le R < 0$:

$$X_{T_r} = X_T - (X_T - \sigma_{1max})\left(\frac{n}{N_1}\right),\ X_{C_r} = X_C - (X_C - |\sigma_{1min}|)\left(\frac{n}{N_1}\right)^k$$

$$Y_{T_r} = Y_T - (Y_T - \sigma_{2max})\left(\frac{n}{N_2}\right),\ Y_{C_r} = Y_C - (Y_C - |\sigma_{2min}|)\left(\frac{n}{N_2}\right)^k \quad (6)$$

$$S_r = S - (S - \sigma_{6max})\left(\frac{n}{N_6}\right).$$

For $R \in (-\infty, -1]$, the same set of Eq. (6) is valid with the exception of the relation for the residual shear strength which is now given by:

$$S_r = S - (S - |\sigma_{6min}|)\left(\frac{n}{N_6}\right) \quad (7)$$

Finally, for $R \in [1, +\infty)$:

$$X_{T_r} = X_T,\ X_{C_r} = X_C - (X_C - |\sigma_{1min}|)\left(\frac{n}{N_1}\right)^k \quad Y_{T_r} = Y_T,\ Y_{C_r} = Y_C - (Y_C - |\sigma_{2min}|)\left(\frac{n}{N_2}\right)^k$$

$$S_r = S - (S - |\sigma_{6min}|)\left(\frac{n}{N_6}\right) \quad (8)$$

$X_{T(C)r}$ and $Y_{T(C)r}$ is the tensile (compressive) residual strength parallel and transverse to the fibres respectively, while S_r is the residual shear strength. σ_{1max}, σ_{2max} and σ_{6max} are the maximum cyclic stresses applied for n cycles and N_i, i=1, 2, 6, the corresponding fatigue life at the specific stress level. In all the above equations for compressive residual strength, expressed by the "sudden death" relation, the exponent k assumes a high value, e.g. 50.

Concerning fatigue strength prediction, it has to be recalled that the methodology used in FADAS is of the ply-to-laminate type with progressive damage modelling. In such an approach failure is considered at the ply level and a static limit condition may be used where however, material strength parameters are replaced by the corresponding residual strength values which are in general functions of the number of cycles and the type of loading. For the cases studied in this work, numerical results were derived by implementing the Puck criteria [6] in the FADAS routine. For the variety of parameters implemented in the limit conditions, guidelines and typical values were given by Puck et al. [7]. The values used in the present version were presented in Table 5 of [13]. Since the criterion is used for cyclic stresses, the lamina strength values given in Table 2 must be replaced by the corresponding residual strength values presented in this section.

4 Constant Life Diagrams and S-N Curves

The life prediction methodology presented herein was introduced for multiaxial VA fatigue. Therefore, characterization of fatigue behaviour in the principal coordinate system of the orthotropic UD ply must take place for several R-values and then by using an appropriate interpolation scheme define the “Constant Life Diagram” or else define the number of cycles to failure, N, for every possible cycle.

A great number of CA cyclic tests were performed [16], [17], [19] and the respective S-N curves parallel, transversely to the fibre and in shear, at three stress ratios R were obtained. The R-ratios for which tests were performed are R=0.1, -1 and 10 which apart from being proposed by wind turbine rotor blade certification bodies as GL or DNV cover a minimum range of fatigue conditions, both in tension and compression. For in-plane shear fatigue strength tests were performed only for R=0.1 and the common assumption that shear strength in the principal material system of an orthotropic

medium does not depend on the sign of the shear stress along with the Goodman approach led to a symmetric CLD. The S-N curves obtained were of the form:

$$\sigma_a = \sigma_o N^{\left(-\frac{1}{k}\right)} \quad (9)$$

In the above relation, σ_a stands for the alternating component of the cyclic stress, N for the number of cycles to failure while constants σ_o and k, depending on the R-ratio and the stress component were given in Table 5.

Table 5: S-N curve parameters for the OB_UD glass/epoxy

	σ_1		σ_2		σ_6	
R	σ_o (MPa)	k	σ_o (MPa)	k	σ_o (MPa)	k
0.1	500.8	10.03	50.2	8.63	38.1	11.06
-1	972.2	8.05	87.5	8.43	N/A	N/A
10	289.5	26.08	88.5	24.32	N/A	N/A

Fatigue behaviour at different stress ratios were obtained by linear interpolation between the already known S-N curves as described by Philippidis and Vassilopoulos [25].

5 FE implementation of FAtigue DAmage Simulator (FADAS)

Constitutive equations and models presented in the previous sections, 2 to 4, form the necessary input data set at the UD ply level. This is all required by FADAS to predict static and fatigue strength, residual strength and stiffness after arbitrary multiaxial VA cyclic loading of any multidirectional laminate made of the basic UD ply. The actual implementation was based on a Glass/Epoxy UD material typical of wind turbine rotor blade applications. For alternative materials, a new data set has to be defined; however

it is believed that most of the existing material models can still be useful for an initial estimation.

Once these data are implemented, the algorithm proceeds by means of FE for the stress analysis using a Reissner-Mindlin shell formulation. With this type of analysis, selected instead of solid 3D modelling to keep computational time realistic, delamination onset and propagation cannot be simulated. A general flowchart of the algorithm is shown in Fig. 9. Further details on the implementation of the various modules shown in the diagram are given in [11].

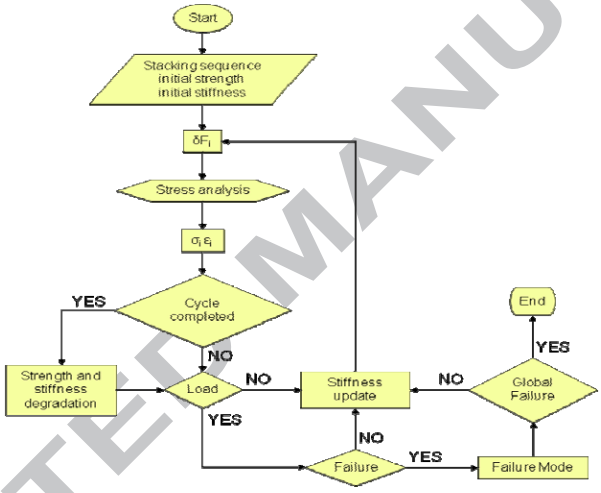

Fig. 9: Flowchart of the FADAS algorithm

6 Conclusions

An anisotropic non-linear constitutive model implementing progressive damage concepts to predict the residual strength/stiffness and life of composite laminates subjected to multiaxial VA cyclic loading was presented. In-plane mechanical properties of the material were fully characterized at the ply level while static or fatigue strength of any multidirectional stacking sequence can be predicted.

The implementation of the method in a commercial FE code, simulating fatigue damage progression in a composite laminate was presented in [11]. Strength and stiffness degradation were modelled using simple and cost-effective schemes, while the failure criterion of Puck along with post failure behaviour of the material, was implemented. The model has been verified through a series of constant amplitude fatigue tests on different lay-ups, simulating a variety of plane stress combinations and failure modes. These results indicated that the FADAS algorithm actually predicts satisfactorily fatigue strength and stiffness degradation under CA loading of prismatic specimens under axial loads.

In its current version, the model has limitations; it neglects the eventual 3D character of the stress and strain fields which could lead to additional failure modes, e.g. delaminations. In addition the viscous nature of the marix material was not taken explicitly into account, thus important effects on actual material performance such as the strain rate and loading frequency or the hygrothermal conditions were also overlooked.

Acknowledgements

Research was funded in part by the European Commission in the framework of the research programme “Integrated Wind Turbine Design (UPWIND), contract No: 019945, SES6. Partial funding was also provided by the General Secretariat of Research and Technology (GSRT) of the Greek Ministry of Development, contract No. F.K. C037.

References

1. Lee JW, Allen DH, Harris CE, Internal state variable approach for predicting stiffness reductions in fibrous laminated composites with matrix cracks. J Compos Mater 1989; **23**, 1273-1291

2. Coats TW, Harris CE, Experimental verification of a progressive damage model for IM7/5260 laminates subjected to tension-tension fatigue. J Compos Mater 1995; **29**(3), 280-305

3. Lo DC, Coats TW, Harris CE, Allen DH, Progressive damage analysis of laminated composite (PDALC). A computational model implemented in the NASA COMET finite element code. *NASA TM-4724,* 1996

4. Shokrieh MM, Lessard LB, Progressive fatigue damage modelling of composite materials, Part I: Modeling. J Compos Mater 2000; **34**(13), 1056-1080

5. Shokrieh MM, Lessard LB, Progressive fatigue damage modelling of composite materials, Part II: Material Characterization and model verification. J Compos Mater 2000; **34**(13), 1081-1116

6. Puck A, Schürmann H, Failure analysis of FPF laminates by means of physically based phenomenological models, Compos Sci Tech 1998; **58**, 1045-1067

7. Puck A, Kopp J, Knops M, Guidelines for the determination of the parameters in Puck's action plane strength criterion, Compos Sci Tech 2002; **62**, 371-378

8. Philippidis TP, Eliopoulos EN, Antoniou AE, Passipoularidis VA, Material Model Incorporating Loss of Strength and Stiffness Due to Fatigue. *UpWind project, Deliverable 3.3.1,* 2007, Contract No.: 019945(SES6)

9. Philippidis TP, Eliopoulos EN, A progressive damage mechanics algorithm for life prediction of composite materials under cyclic complex stress, in *Fatigue life prediction of composites and composite structures,* ed. A. P. Vassilopoulos, Woodhead Publishing Ltd and CRC Press, 2010, Chapter 11, 390-436

10. Passipoularidis VA, Philippidis TP, Brøndsted P, Fatigue life prediction in composites using progressive damage modeling under block and spectrum loading, Int J Fatigue 2011; **33**, 132-144

11. Eliopoulos EN, Philippidis TP, A progressive damage simulation algorithm for GFRP composites under cyclic loading. Part II: FE implementation and model validation, Compos Sci Tech, submitted for publication (2010)

12. Jacobsen, T.K. (2002). Reference material (OPTIMAT). Glass-Epoxy, OB_SC_R001_LM, (http://www.wmc.eu/optimatblades.php)

13. Antoniou AE, Kensche CW, Philippidis TP. Mechanical behavior of glass/epoxy tubes under combined static loading. Part II: Validation of FEA progressive damage model. Compos Sci Tech 2009; **69**(13):2248–55

14. Megnis M, Brøndsted P, Measurements of in-plane shear properties of GEV206 at ambient room conditions using V-notched beam test specimen. OB_TG3_R009, 2003. (http://www.wmc.eu/optimatblades.php)

15. Richard RM, Blacklock JR, Finite element analysis of inelastic structures. *AIAA*, 1969; **7**, 432-438

16. Philippidis TP, Assimakopoulou TT, Antoniou AE & Passipoularidis VA, Fatigue tests on OB standard coupons at 90^{o} Main test phase I. OB_TG2_R021, 2005 (http://www.wmc.eu/optimatblades.php)

17. Philippidis TP, Assimakopoulou TT, Passipoularidis VA & Antoniou AE, Static and fatigue tests on ISO standard ±45˚ coupons Main test phase I. OB_TG2_R020, 2004 (http://www.wmc.eu/optimatblades.php)

18. Nijssen RPL, Knowledge Centre WMC, Wieringerwerf, The Netherlands, personal communication 2007

19. Philippidis TP, Passipoularidis VA, Assimakopoulou TT & Antoniou AE, Fatigue tests in the fiber direction of UD OB standard specimen Main test phase I. OB_TG1_R013, 2006 (http://www.wmc.eu/optimatblades.php)

20. Philippidis TP, Passipoularidis VA, Residual strength after fatigue in composites: Theory vs. experiment, Int J Fatigue 2007; **29**, 2104-2116

21. Passipoularidis VA, Philippidis TP, Strength Degradation due to Fatigue in Fiber Dominated Glass/Epoxy Composites: A Statistical Approach, J. Compos Mater 2009; **43**(9), 997-1013

22. Nijssen RPL, Fatigue life prediction and strength degradation of wind turbine rotor blade composites, 2006, PhD Thesis, Faculty of Aerospace Engineering, T. U. Delft

23. Passipoularidis VA, Philippidis TP, A study of factors affecting life prediction of composites under spectrum loading, Int J Fatigue 2009; **31**(3), 408-417

24. Broutman LJ, Sahu S, A new theory to predict cumulative fatigue damage in fibreglass reinforced plastics, *Composite materials: Testing and design (2nd conference)* ASTM STP 497, 1972, 170-188

25. Philippidis TP, Vassilopoulos AP, Life prediction methodology for GFRP laminates under spectrum loading, Compos: Part A 2004; **35**(6), 657-666